Electrochemical and
Solid-State Letters

Atomic Layer Deposition of RuAlO Thin Films as a Diffusion Barrier for Seedless Cu Interconnects

Electrochemical and Solid-State Letters, **14** (5) D57-D61 (2011)
1099-0062/2011/14(5)/D57/5/$28.00 © The Electrochemical Society

Atomic Layer Deposition of RuAlO Thin Films as a Diffusion Barrier for Seedless Cu Interconnects

Taehoon Cheon,[a] Sang-Hyeok Choi,[a] Soo-Hyun Kim,[a,*,z] and Dae-Hwan Kang[b]

[a]*School of Materials Science and Engineering, Yeungnam University, 214-1, Dae-dong, Gyeongsan-si 712-749, Korea*
[b]*Samsung Electronics Corporation Ltd., Memory Division, Semiconductor Business, Yongin-City, Gyeonggi-Do 446-711, South Korea*

Ruthenium (Ru)-based ternary thin films (RuAlO) were prepared by thermal atomic layer deposition (ALD) with repeated super-cycles consisting of Ru and Al_2O_3 ALD sub-cycles at 225°C. The step coverage of ALD-RuAlO was excellent, around 93% at contact holes with an aspect ratio of ~29 (top-opening diameter: ~74 nm). Transmission electron microscopy analysis showed that RuAlO films formed with non-columnar grains and a nano-crystalline microstructure consisting of Ru nano-crystals separated by amorphous Al_2O_3. The sheet resistance and X-ray diffraction showed that the structure of Cu (100 nm)/RuAlO (15 nm)/Si was stable after annealing at 650°C for 30 min. Fifty nanometer-thick Cu was electrodeposited directly on RuAlO film, suggesting that it could be a viable candidate as a Cu direct plateable diffusion barrier.
 [DOI: 10.1149/1.3556980]

Manuscript submitted January 3, 2011; revised manuscript received January 26, 2011. Published March 8, 2011.

The current structure of Cu interconnects consists of electroplated (EP)-Cu that is responsible for the most of the current and an underlying stack of a relatively high-resistive Ta/TaN diffusion barrier and Cu seed layer for the Cu EP process, which is deposited mostly by physical vapor deposition (PVD).[1] However, with the continuous scaling-down of devices, the filling of EP-Cu into patterned features becomes increasingly difficult, which is aggravated by the underlying thick diffusion barrier and seed layer. Moreover, an unwanted and drastic increase in Cu wire resistance occurs due to the size effect on the resistivity of metal films.[2,3] Both problems can be addressed by increasing the volume of EP-Cu filled in the patterned features by the direct plating of Cu because the EP of Cu can be achieved on a diffusion barrier without a seed layer. The conformality, thickness controllability, and large-area uniformity of the process for a Cu direct-plateable diffusion barrier need to be considered due to continuous scaling of the devices. Atomic layer deposition (ALD) is a viable solution for depositing a Cu direct-plateable diffusion barrier because it employs a self-limiting film growth mode through surface-saturated reactions, which enables atomic-scale control of the film thickness with excellent step coverage.[4]

Ru has been suggested as a diffusion barrier for seedless Cu interconnects.[5,6] In addition, Ru films have been grown successfully by ALD using a variety of Ru metallorganic precursors with excellent step coverage.[7–12] However, Ru itself is not a suitable diffusion barrier against Cu due mainly to its poor microstructure with polycrystalline columnar grains.[13,14] Indeed, many studies demonstrated that the microstructure plays an important role in the resulting diffusion barrier performance.[15] Two types of approaches were reported to address the poor diffusion barrier performance and obtain reliable seedless Cu interconnects with Ru. The first is to use Ru as a seed layer and combine it with superior materials to function as a diffusion barrier against Cu. Sputtered–deposited Ru/TaN,[16] Ru/Ta,[17] Ru/WN_x[14] bilayers, and atomic layer deposited Ru/TaCN bilayer[18] have been suggested and their diffusion barrier performance against Cu were superior to a Ru single layer with the same thickness. Nevertheless, bilayer diffusion barriers require additional process that can increase the processing cost. Moreover, the volume of the trench for Cu to be filled becomes narrow due to the additional materials prior to the EP of Cu. The second approach is to modify the microstructure of Ru to an amorphous or nanocrystalline structure. A basic idea is to incorporate materials into Ru during deposition to produce Ru-based multicomponent films. Ru-TiN,[19] Ru-TaN,[20] Ru-WCN,[21] and RuSiN[22] films were suggested and the successful direct plating of Cu on them was also reported. However, all reports on them used plasma-enhanced ALD. Generally, the conformality of plasma-based process is more limited due to the high probability of surface recombination of reactive radicals in higher aspect structures.[23,24] In this study, Ru-based ternary thin films were developed using a thermal ALD process. ALD-Al_2O_3 was incorporated into ALD-Ru to prevent its columnar growth, and a ternary thin film, RuAlO, with a nanocrystalline and non-columnar grain structure, was fabricated at 225°C. Finally, its diffusion barrier performance against Cu was compared with ALD-Ru.

ALD-RuAlO films were deposited on SiO_2 (100 nm)/Si and TiN (20 nm)/SiO_2 (100 nm)/Si using a traveling wave-type thermal ALD reactor (Lucida-D100, NCD Technology, Korea) at a deposition temperature of 225°C and pressure of 1 Torr. RuAlO films were deposited by repeating the super-cycles consisting of Ru and Al_2O_3 ALD sub-cycles. Each sub-cycle consisted of several unit cycles. A single unit cycle was comprised of a precursor injection pulse, a purge pulse, a reactant injection pulse, and another purge pulse. IMBCHRu [(η6−1-Isopropyl−4-methylbenzene) (η4−cyclohexa-1, 3-diene) ruthenium (0), $C_{15}H_{22}Ru$] and trimethylaluminum [TMA, $(CH_3)_3Al$] were used as the Ru and Al_2O_3 precursors, respectively. Molecular O_2 and water vapor were used as the reactants for the Ru and Al precursor, respectively. The temperature of the canisters containing IMBCHRu, TMA and water were kept at 120, 10 and 10°C, respectively. A zero metal valence Ru precursor was used because a previous study reported that it could improve significantly the nucleation of ALD-Ru on a SiO_2 surface,[12] which is important, particularly when the Ru-based ALD process is applied to the nano-scale regime. The pulse time of IMBCHRu and TMA was varied from 1 to 12 s and 0.1 to 2 s, respectively, to determine the precursor pulse times to guarantee self-limiting film growth. N2 as a purge gas was flowed for 10 s immediately after injecting the precursors, O_2 molecules and water vapor. The intermixing ratios of Ru and Al_2O_3 in the deposited films could be controlled by changing the number of unit cycles in an Al_2O_3 sub-cycle, whereas the number of unit cycles allocated for a Ru sub-cycle was fixed to 40 cycles. The number of total super-cycles was five, which means that the total cycles of ALD-Ru was 200.

First, the Ru and Al_2O_3 ALD processes were characterized. The growth rate of the Ru and Al_2O_3 films were determined from the thickness with the deposition condition using cross-sectional view transmission electron microscopy (XTEM, Tecnai F20 equipped with 200 kV accelerating voltage and field emission gun). The composition of ALD-Ru and ALD-Al_2O_3 was characterized by secondary ion mass spectrometry (SIMS, CAMECA IMS-6f in Korea Basic Science Institute) and Auger electron spectroscopy (AES) depth profiling, respectively. The SIMS results on ALD-Ru were calibrated by Rutherford backscattering spectrometry (RBS). The incorporation of Al and O into Ru was also confirmed by SIMS. The properties of the RuAlO films were analyzed comparatively to the

* Electrochemical Society Active Member.
z E-mail: soohyun@ynu.ac.kr

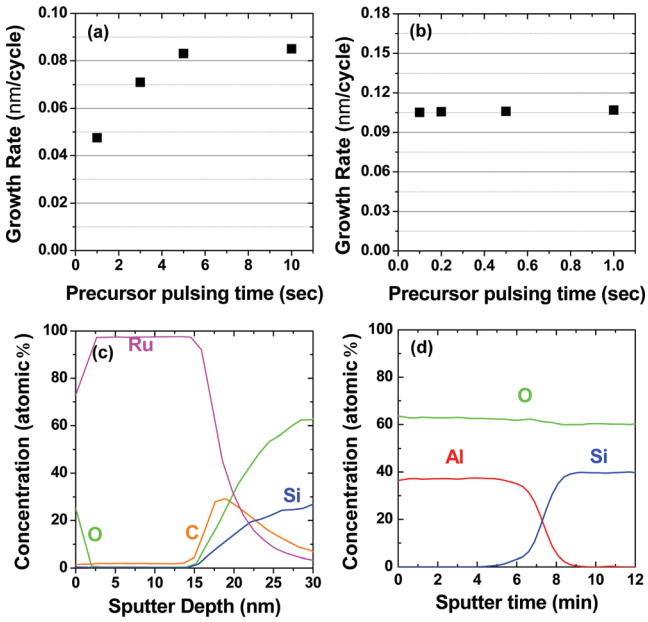

Figure 1. (Color online) (a) Growth rate of ALD-Ru process as a function of the Ru precursor pulsing time, (b) growth rate of ALD-Al_2O_3 process as a function of the Al precursor pulsing time, (c) SIMS depth profiles of ALD-Ru film, and (d) AES depth profile of ALD-Al_2O_3 film.

Ru counterpart to determine the effect of Al_2O_3 addition to Ru. Plan-view TEM and XTEM were used to examine the microstructures of the Ru and RuAlO films. The step coverage of the ALD-RuAlO films were evaluated at the contacts with an aspect of ~29 (top opening diameter: ~74 nm). The diffusion barrier performance of RuAlO film between Cu and Si was evaluated. One hundred-nanometer-thick Cu films were deposited onto 15-nm-thick RuAlO-covered Si wafers by sputtering. The Cu/RuAlO/Si samples were then annealed in a high vacuum ($< 2 \times 10^{-6}$ Torr) for 30 min at temperatures ranging from 450 to 700°C at 50°C intervals. The barrier performances were evaluated by sheet resistance measurements and x-ray diffraction (XRD) after annealing. Finally, Cu was electrodeposited directly onto an 10 nm-thick RuAlO ALD-RuAlO film to test the feasibility of the film as a diffusion barrier for seedless Cu interconnects. The detailed condition for the EP of Cu could be found elsewhere.[12]

The effect of the precursor pulse time for Ru and Al_2O_3 was examined. Ru growth was self-limited with a precursor pulsing of 5 s, whereas Al_2O_3 growth was self-limited with only a 0.1 s precursor pulse, as shown in Figs. 1a and 1b. The growth rates of Ru and Al_2O_3 ALD were 0.084 and 0.105 nm/cycle, respectively. Figure 1c shows the SIMS depth profile of ALD-Ru film deposited on SiO_2. Although the process was performed using O_2 gas, no oxygen was incorporated into the film. A very little amount of carbon (~1.8 atom %) was incorporated into the film, indicating that O_2 was a very effective reactant for reducing IMBCHRu to Ru. We considered that the large amount of carbon at the interface between SiO_2 and ALD-Ru was mainly due to the artifact of SIMS analysis rather than substrate contamination prior to deposition. Structural analysis by XRD and electron diffraction[12] showed that the film consisted of hexagonal-close-packed (HCP) Ru with no tetragonal RuO_2 phase. The resistivity of Ru was approximately 40 μΩ cm. Figure 1d shows the AES depth profile of ALD-Al_2O_3. We could not detect carbon in the Al_2O_3 film, indicating water vapor is an effective reducing agent for TMA. The AES results showed that the film is O-rich Al_2O_3, its composition was determined as $Al_2O_{3.37}$.

From these results, one Ru ALD unit cycle was set as IMBCHRu pulse (5 s) – N_2 purge (10 s) – O_2 pulse (0.5 s) – N_2 purge (10 s), and one Al_2O_3 ALD unit cycle was set as TMA (0.2 s) pulse – N_2 purge (10 s) –H_2O pulse (0.2 s) – N_2 purge (10 s) for preparing a RuAlO film, and various RuAlO thin films could be prepared with a different number of Ru and Al_2O_3 unit cycles as shown schematically in Fig. 2a. Figure 2b shows the secondary ion intensities of the RuAlO film deposited on a SiO_2 substrate from SIMS depth profiling. Here, the number of ALD-Al_2O_3 unit cycles was three. The secondary ion intensities from Al and O in the film suggest that Al_2O_3 had been incorporated successfully in the Ru film by the addition of ALD-Al_2O_3 cycles cyclically to Ru ALD cycles.

The relevant films were analyzed by TEM to confirm the phase and characterize the microstructure of the RuAlO films in detail. For comparison, TEM analysis was performed on ALD-Ru film. The plan-view TEM bright-field (BF) image Fig. 3a of the ALD-Ru film shows crystalline grains with a size of approximately 10–20 nm. Grain boundaries are clearly observed between the Ru grains. Corresponding selected-area electron diffraction analysis (the inset of Fig. 3a) revealed a spotty pattern, confirming that the ALD-Ru formed randomly-oriented polycrystalline grains. Indexing of the diffraction pattern indicated that the film formed HCP crystalline Ru. The ALD-Ru film formed a columnar microstructure, where the grain boundaries were vertical with respect to the TiN substrate, as shown by the cross-sectional view TEM image (Fig. 3b). The plan-view TEM image of ALD-RuAlO film (Fig. 3c) showed that relatively dark-contrast grains, ~3 nm in size, are distributed uniformly with bright-contrast regions separating the dark-contrast grains. The corresponding selected-area electron diffraction pattern (the inset of Fig. 3c) was less spotty and formed a ring-type pattern, showing that the sizes of the crystal grains were reduced significantly compared to those of the Ru counterpart. This is closely matched with that of HCP-Ru, indicating that the grains with dark-contrast shown in

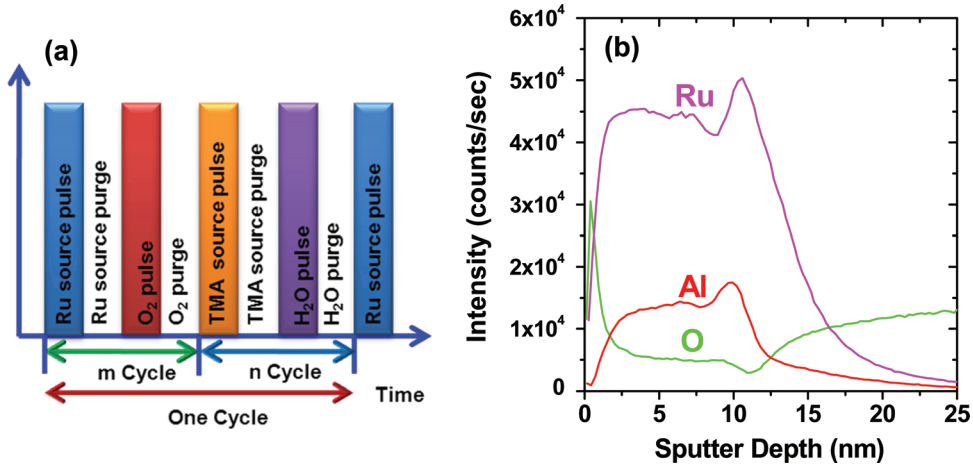

Figure 2. (Color online). (a) Schematic diagram of the process sequence on ALD-RuAlO and (b) SIMS depth profile of RuAlO film (number of ALD-Ru subcycles: 40 and number of ALD-Al_2O_3 subcycles: 3).

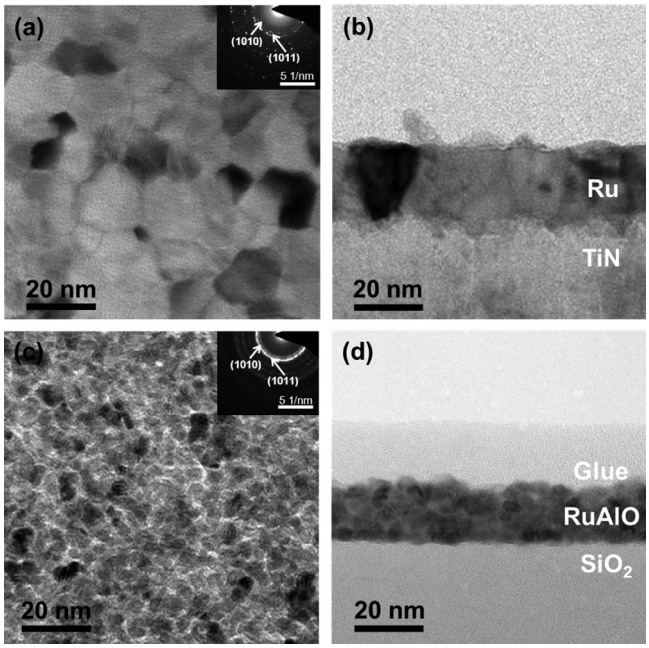

Figure 3. (a) Plan-view, (b) cross-sectional view TEM (XTEM) image of ALD-Ru film, (c) plan-view, and (d) XTEM image of ALD-RuAlO film.

TEM image are crystalline Ru. The cross-sectional view TEM image of ALD-RuAlO (Fig. 3d) is quite different from to that of ALD-Ru. The layered structure of Ru/Al_2O_3 was not observed but nano-crystals with dark contrast appear to be embedded into regions with brighter contrast. Plan-view TEM analysis (data not shown here) showed that the ALD-Ru film deposited by 40 ALD cycles was not continuous. In addition, the periodic addition of three Al_2O_3 ALD cycles between Ru growth, which was not sufficient for making continuous Al_2O_3 films, produced amorphous Al_2O_3 both on the Ru nanocrystals and the open regions between them. Considering both SIMS results (Fig. 2b) and the mass contrast of the TEM image, it is believed that the bright region separating the Ru nanocrystals was amorphous Al_2O_3. Finally, the columnar grain structure of Ru was destroyed and dense amorphous Al_2O_3 was filled between Ru nanocrystals. The formation of this type of microstructure by the incorporation of Al_2O_3 into Ru will provide better performance as a diffusion barrier against Cu compared to the Ru counterpart, which has a columnar grain structure to give a fast pathway for Cu diffusion.

Figures 4a–4c shows the change in step coverage of the ALD-RuAlO film at the contact hole formed in the SiO_2 layer with an aspect ratio of ~29 (top-opening diameter: ~74 nm and contact height: ~2150 nm). Here, the number of Al_2O_3 unit cycles was three. The step coverage was almost perfect in these ultra high aspect ratio contact holes. The XTEM images of the top (Fig. 4a), middle (Fig. 4b) and bottom (Fig. 4c) of the contact showed that the thickness of the ALD RuAlO was between ~14.2 and ~15.3 nm. This gives step coverage of 93% (defined by the bottom thickness/top thickness). The excellent step coverage of RuAlO was attributed to the ideal ALD growth of Ru and Al_2O_3 without partial decomposition of the precursors, as shown in Figs. 1a and 1b. Indeed, the step coverage of the Ru film at the same contact holes (Figs. 4d–4f) was excellent under the growth condition used in this study and that of ALD-Al_2O_3 was also excellent, as shown in Figs. 4g–4i.

Figure 5a shows the changes in the sheet resistance of the Cu (100 nm)/RuAlO (15 nm)/Si wafer samples as a function of the annealing temperature. The sheet resistance mainly represents the conditions and quantities of the Cu layer because it carries most of the sensor current. The sheet resistance contributions from RuAlO can be neglected because of its much higher resistivity (~210 μΩ cm) and thinner thickness than Cu. The sheet resistances of the multilayer samples were not higher than that of the as-deposited sample

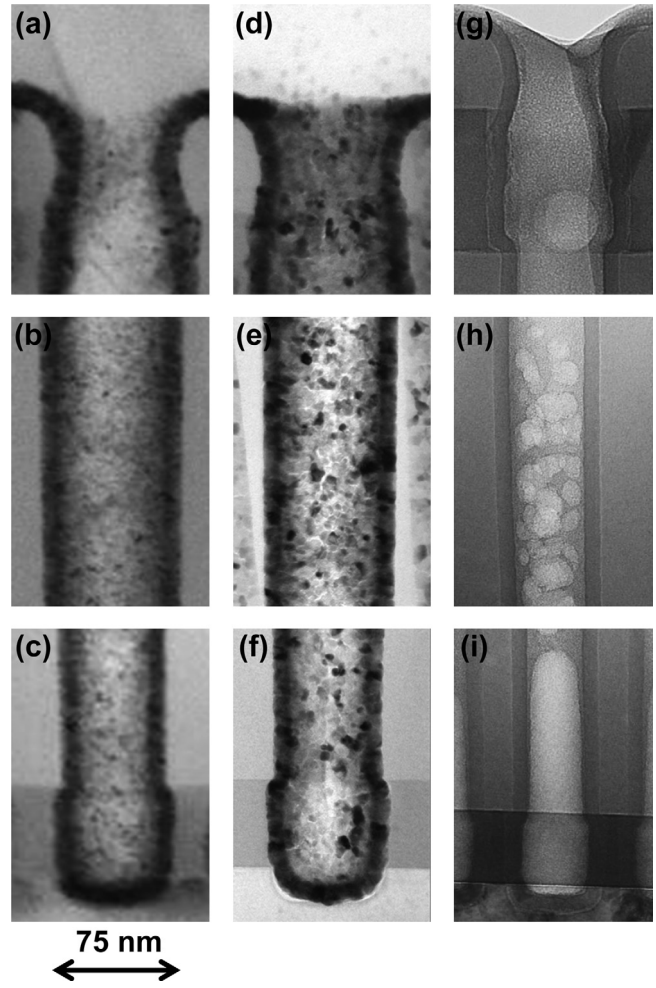

Figure 4. XTEM images to show the step converges of ALD-RuAlO, ALD-Ru, and ALD-Al_2O_3; (a) XTEM image on ALD-RuAlO at the top, (b) middle, (c) bottom of the contact, (d) XTEM image on ALD-Ru at the top, (d) middle, (f) bottom of the contact, (g) XTEM image on ALD-Al_2O_3 at the top, (h) middle, and (i) bottom of the contact. The aspect ratio of the contact is ~29 and the top opening diameter is ~74 nm.

until annealing at 650°C. Annealing below 650°C resulted in a decrease in sheet resistance, probably due to the increase in the grain size of the Cu films and defect annihilation in the Cu film. The sheet resistance increased abruptly after annealing at 700°C. XRD analysis of the annealed samples was performed to explain the increase in sheet resistance of the multilayer structure. Figure 5b shows the corresponding XRD results for the annealed samples. In the case of the as-deposited Cu (100 nm)/RuAlO (15 nm)/Si sample, peaks from face-centered-cubic (FCC) Cu, and the Si substrate were detected. XRD clearly shows that the initial multilayer structure of Cu (100 nm)/RuAlO (15 nm)/Si is preserved until annealing at 650°C, and the intensities of the peaks from Cu increased, indicating an increase in the grain sizes of Cu with annealing. The peaks from Ru [$(10\bar{1}0)$, $2\theta = 38.57°$ and (1013), $2\theta = 78.47°$] developed, indicating that the grains sizes of Ru in the RuAlO film increased with annealing. This also shows that Cu silicides ($2\theta = 45.19°$) are first detected after annealing at 650°C but the intensity is weak, and strong Cu peaks are still observed. This suggests that Cu diffusion into Si to form Cu silicide is not severe. Indeed, the sheet resistance was not increased after annealing at 650°C, as shown in Fig. 5a. When the annealing temperature was increased to 700°C, where the sudden increase in sheet resistance was observed, various types of Cu silicides were detected with a decrease in the Cu peak, even though the dominant Cu silicide formed was η''-Cu_3Si. This

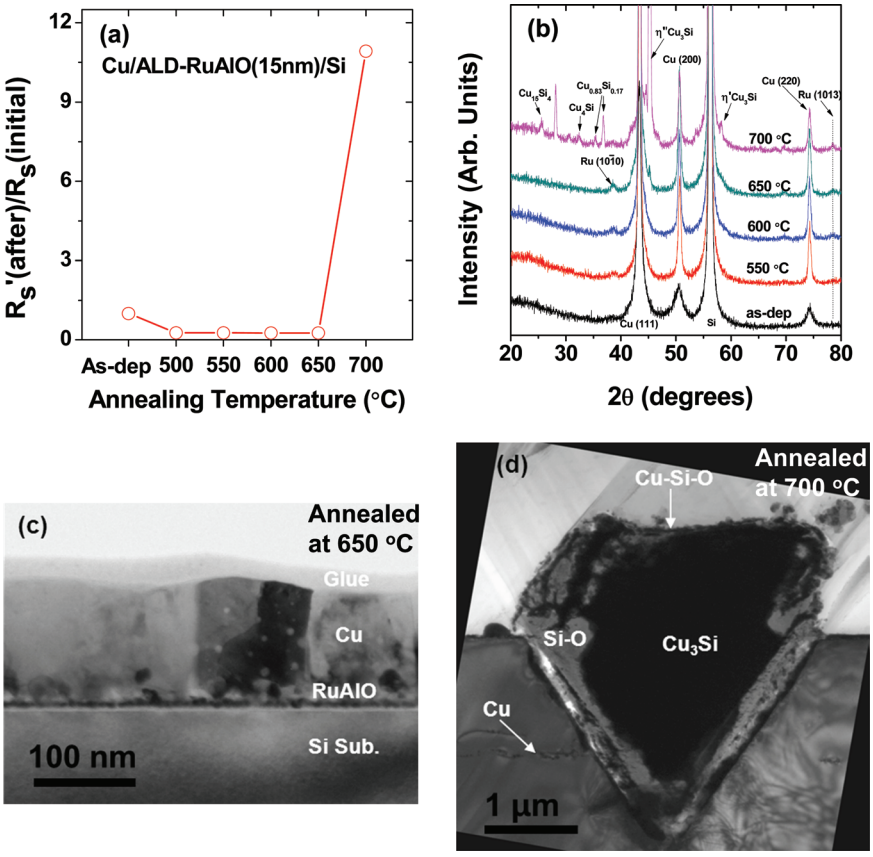

Figure 5. (Color online). (a) The change in the ratios of the sheet resistances of Cu (100 nm)/ALD-RuAlO (15 nm)/Si structures before and after annealing, (b) glazing angle XRD results of Cu (100 nm)/ALD-RuAlO (15 nm)/Si structures as a function of the annealing temperature, (c) XTEM image of Cu (100 nm)/ALD-RuAlO (15 nm)/Si structures after annealing at 650°C, and (d) 700°C.

suggests that the drastic increase in sheet resistance is caused mainly by the consumption of Cu and the formation of Cu silicide via the diffusion of Cu into Si through RuAlO, which has a much higher resistivity than Cu.[25] The improved diffusion barrier performance of RuAlO against Cu is due to its nano-crystalline non-columnar structure, which extends the length of the rapid diffusion path of Cu, such as grain boundaries, compared to the columnar grain structure of Ru.

Figure 5c shows a XTEM image of the sample annealed at 650°C. Although the Cu silicides were detected in the annealed sample at this temperature from XRD analysis, no Cu silicide was obtained from XTEM analysis. This suggests that the failure of a RuAlO diffusion barrier at 650°C occurred locally and was not severe. In the sample annealed at 700°C (Fig. 5d), a new triangular shaped phase was formed. This was identified as a η''-Cu_3Si phase from energy dispersive spectroscopy (EDS) and electron diffraction. However, RuAlO still preserved its layer at the location where failure occurred. This result indicated that ALD-RuAlO diffusion barrier failed between Cu and Si by the diffusion of Cu through the RuAlO, resulting in the formation of crystalline defects in the Si or Cu silicides not by the interfacial reactions between the barrier layer and adjacent layers. Finally, we tested a possibility of Cu direct plating on 10 nm-thick ALD-RuAlO film deposited with the Al_2O_3 unit cycles of 3. Cross-sectional view scanning electron microscopy analysis (not shown here) confirmed that Cu films as thin as ~50 nm were successfully and continuously grown on ALD-RuAlO film by electroplating. This indicated that Cu nuclei were formed very fast during the electroplating on ALD-RuAlO film.

Summary and Conclusions

Ru-based ternary thin films, RuAlO, were prepared by thermal ALD by combining ALD-Ru and ALD-Al_2O_3 processes at 225°C as a diffusion barrier for seedless Cu interconnects. TEM analysis showed that a RuAlO film formed with non-columnar grains and a nano-crystalline microstructure consisting of Ru nano-crystals separated by amorphous Al_2O_3, whereas the Ru films were polycrystalline with columnar grains. The step coverage of ALD-RuAlO was excellent, around 93% at contact holes with an aspect ratio of ~29. The sheet resistance measurements and XRD showed that the structure of Cu (100 nm)/RuAlO (15 nm)/Si was stable after annealing at 650°C for 30 min, whereas the Cu (100 nm)/Ru (15 nm)/Si structure failed after annealing at 45°C.[14] An excellent barrier property of ALD-RuAlO for blanket film indicates that it would have superior properties in device structures because of its inherent good conformality. The electroplating of Cu was achieved on a very thin (10-nm-thick) RuAlO film. Therefore, the ALD-RuAlO thin film developed in this study can be a viable candidate as a diffusion barrier for seedless Cu interconnects, and will be beneficial in reducing the increase in resistance in Cu wiring caused by the size effect. But, it should be indicated that the diffusion barrier investigated in this study is quite thick to directly apply for the future Cu interconnect. Thus, further studies with a thinner thickness are being investigated and will be reported in near future.

Acknowledgments

This work was supported by the Technology Innovation Program (Industrial Strategic technology development program, 10035430, Development of reliable fine-pitch metallization technologies) funded by the Ministry of Knowledge Economy (MKE, Korea).

References

1. D. Edelstein, C. Uzoh, C. Cabral, Jr., P. DeHaven, P. Buchwalter, A. Simon, E. Cooney III, S. Malhotra, D. Klaus, H. Rathore, et al., in *Advanced Metallization Conference in 2001*, A. J. McKerrow, Y. Shacham-Diamand, S. Zaima, and T. Ohba, Editors, pp. 541–547, Materials Research Society Symposium Proceedings, Warrendale, PA (2002).
2. S. M. Rossnagel and T. S. Kuan, *J. Vac. Sci. Technol. B*, **22**, 240 (2004).

3. W. Steinhögl, G. Schindler, G. Steinlesberger, and M. Engelhardt, *Phys. Rev. B*, **66**, 075414 (2002).
4. H. Kim, H.-B.-R. Lee, and W.-J. Maeng, *Thin Solid Films*, **517**, 2563 (2009).
5. D. Josell, D. Wheeler, C. Witt, and T. P. Moffat, *Electrochem. Solid-State Lett.*, **6**, C143 (2003).
6. M. W. Lane, C. E. Murray, F. R. McFeely, P. M. Vereecken, and R. Rosenberg, *Appl. Phys. Lett.*, **83**, 2330 (2003).
7. T. Aaltonen, P. Alën, M. Ritala, and M. Leskelä, *Chem. Vap. Deposition*, **9**, 45 (2003).
8. T. Aaltonen, M. Ritala, K. Arstila, J. Keinonen, and M. Leskelä, *Chem. Vap. Deposition*, **10**, 217 (2004).
9. O.-K. Kwon, J.-H. Kim, H.-S. Park, and S.-W. Kang, *J. Electrochem. Soc.*, **151**, G109 (2004).
10. S.-K. Kim, S. Y. Lee, S. W. Lee, G. W. Hwang, C. S. Hwang, J. W. Lee, and J. Jeong, *J. Electrochem. Soc.*, **154**, D95 (2007).
11. H. Li, D. B. Farmer, R. G. Gordon, Y. Lin, and J. Vlassak, *J. Electrochem. Soc.*, **154**, D642 (2007).
12. T.-K. Eom, W. Sari, K.-J. Choi, W.-C. Shin, J.-H. Kim, D.-J. Lee, K.-B. Kim, H. Sohn, and S.-H. Kim, *Electrochem. Solid-State Lett.*, **12**, D85 (2009).
13. T. N. Arunagiri, Y. Zhang, O. Chyan, M. El-Bouanani, M. J. Kim, K. H. Chen, C. T. Wu, and L. C. Chen, *Appl. Phys. Lett.*, **86**, 083104 (2005).
14. W. Sari, T.-K. Eom, C.-W. Jeon, H. Sohn, and S.-H. Kim, *Electrochem. Solid-State Lett.*, **12**, H248 (2009).
15. A. E. Kaloyeros and E. Eisenbraun, *Annu. Rev. Mater. Sci.*, **30**, 363 (2000).
16. X.-P. Qu, J.-J. Tan, M. Zhou, T. Chen, Q. Xie, G.-P. Ru, and B.-Z. Li, *Appl. Phys. Lett.*, **88**, 151912 (2006).
17. J.-J. Tan, X.-P. Qu, Q. Xie, Y. Zhou, and G.-P. Ru, *Thin Solid Films*, **504**, 231 (2006).
18. S.-H. Kim, H.-T. Kim, S.-S. Yim, D.-J. Lee, K.-S. Kim, H.-M. Kim, K.-B. Kim, and H. Sohn, *J. Electrochem. Soc.*, **155**, H589 (2008).
19. S.-W. Kim, S.-H. Kwon, S.-J. Jeong, and S.-W. Kang, *J. Electrochem. Soc.*, **155**, H885 (2008).
20. S. Kumar, D. Greenslit, T. Chakraborty, and E. T. Eisenbraun, *J. Vac. Sci. Technol. A*, **27**, 572 (2009).
21. D. Greenslit, S. Kumar, T. Chakraborty, and E. T. Eisenbraun, *ECS Trans.*, **13** (8), 63 (2008).
22. T.-K. Eom, S.-H. Kim, K.-S. Park, S. Kim, and H. Kim, *Electrochem. Solid-State Lett.*, **14**, D10 (2011).
23. J. Dendooven, D. Deduytsche, J. Musschoot, R. L. Vanmeirhaeghe, and C. Detavernier, *J. Electrochem. Soc.*, **157**, G111 (2010).
24. Y.-B. Jiang, N. Liu, H. Gerung, J. L. Cecchi, and C. Jeffrey Brinker, *J. Am. Chem. Soc.*, **128**, 11018 (2006).
25. M. O. Aboelfotoh and L. Krusin-Elbaum, *J. Appl. Phys.*, **70**, 3382 (1991).